

Determination of key soil characteristic parameters using angle of repose and direct shear stress test

Qizhi Yang^{1,2*}, Lei Shi¹, Aiping Shi^{1,2}, Mingsheng He¹, Xiaoqi Zhao¹, Li Zhang¹, Min Addy^{3*}

(1. School of Agricultural Engineering, Jiangsu University, Zhenjiang 212013, Jiangsu, China;

2. China Wine Industry Technology Institute, Yinchuan 750021, China;

3. Department of Bioproducts and Biosystems Engineering, University of Minnesota, MN 55108, USA)

Abstract: Discrete element modelling (DEM) is a numerical method for examining the dynamic behavior of granular media. In order to build an accurate simulation model and provide more comprehensive soil characteristic parameters for the design and optimization of various soil contact machinery, in this paper, the discrete element simulation method (EDEM) combined with experimental approach is used to investigate the soil contact characteristic parameters in East Asia. In this study, Hertz-Mindlin (no slip) was used as a particle contact model by taking particle contact parameters and soil JKR (Johnson-Kendall-Roberts) surface energy as determinants, and repose angle, internal friction angle, and cohesive force as evaluation indexes. The method of Plackett-Burman, Steepest ascent, and Box-Behnken were used to gradually reduce the range of parameters needed for simulation until the most accurate value was determined. The results show that the restitution coefficient, static friction coefficient, and rolling friction coefficient between soil particles have significant effects on the DEM model, and their value of them are 0.596, 0.725, and 0.16, respectively. Based on these parameters used for the repose angle test and direct shear stress test, the value of repose angle is 31.97°, the internal friction angle is 27.61°, and the cohesive force is 33.06 kPa. The relative errors with the actual measured values are 9.54%, 1.87%, and 2.31%, respectively. In order to further test whether the simulation parameters of soil obtained by repose angle test and direct shear stress test are consistent with the real soil, comparison test between field test and discrete element simulation was used. The results show that the error in height of ridge between the simulated soil and the actual soil is 4.06%, which is within the acceptable range. It also indicates that the calibrated and optimized soil simulation model can accurately represent the real soil. The research provides theoretical basis and technical support for the study of soil contact parts by using the discrete element method, combined with repose angle test and direct shear stress test.

Keywords: soil, characteristic parameters, calibration, repose angle, direct shear stress, discrete element

DOI: 10.25165/j.ijabe.20231603.6293

Citation: Yang Q Z, Shi L, Shi A P, He M S, Zhao X Q, Zhang L, et al. Determination of key soil characteristic parameters using angle of repose and direct shear stress test. *Int J Agric & Biol Eng*, 2023; 16(3): 143–150.

1 Introduction

The discrete element method (DEM) is a numerical method used to analyze and solve the dynamic problems of complex discrete systems. It is widely used in the simulation of granular structures^[1]. Due to the complexity of soil properties, there is no certain rule to describe the mechanical properties of the soil. The ordinary finite element soil model has great limitations and can be only used for simulating soil damage behavior, but not the soil movement process^[2]. The discrete element method is a better option because it can integrate soil particle contact mechanics model,

therefore can be used to simulate the micro and macro deformation of particles and the interaction between soil and machine. The discrete element method provides more accurate soil models, that can be used as a theoretical basis for designing and optimizing soil contacting parts in agricultural machineries.

The key to building an accurate DEM model is to obtain accurate soil parameters, including intrinsic parameters, material contact parameters, and contact model parameters^[3-6]. The intrinsic parameters of particles can be obtained by general test methods, but the contact parameters are difficult to obtain through experiments. Therefore, many scholars have studied the calibration of particle simulation parameters. Hertz Mindlin (no slip) is suitable for soils with high dispersion, small particles, and little difference in structure and shape. Hu et al.^[7] calculated the movement and distribution of sediment particles in the ground effect by combining Hertz-Mindlin (no slip) and Hertz-Mindlin with JKR (Johnson-Kendall-Roberts) contact model. Ucgul et al.^[8,9] calibrated simulation parameters of cohesive and non-cohesive soils by combining Hertz-Mindlin (no slip) and Hysteretic spring contact model, so as to provide the basis for the plastic deformation of soil under stress. Chen et al.^[10] and others used the Hertz-Mindlin bonding model to simulate the agglomerative and cohesive properties of agricultural soils. Wu et al.^[11] used Hertz-Mindlin with JKR contact model and Box-Behnken method to simulate the angle of repose, and calibrated the simulation parameters of sandy loam

Received date: 2020-11-23 **Accepted date:** 2023-02-23

Biographies: Lei Shi, ME, research interest: agricultural machinery, Email: 525264834@qq.com; Aiping Shi, ME, Professor, research interest: auto intelligent management system, Email: shap@ujs.edu.cn; Mingsheng He, ME, research interest: agricultural machinery, Email: hms5456@163.com; Xiaoqi Zhao, ME, research interest: agricultural machinery, Email: 1145193547@qq.com; Li Zhang, MS, research interest: agricultural ecology, Email: 754381745@qq.com.

***Corresponding author:** Qizhi Yang, PhD, Professor, research interest: agricultural robots, field management machinery. Jiangsu University, Zhenjiang 212013, China. Tel: +86-13815172929, Email: yangqz@ujs.edu.cn; Min Addy, PhD, Professor, research interest: agricultural robots, agricultural machinery. Department of Bioproducts and Biosystems Engineering, University of Minnesota, 2004 Folwell Ave, St. Paul, MN 55108, USA. Tel: +1-612-6255200, Email: minxx039@umn.edu.

soil. Based on soil repose angle test, Xiang et al.^[12] used Hertz-Mindlin with JKR contact model to calibrate the simulation parameters of clay loam. Although many scholars have made many explorations on the method to calibrate parameters used for DEM soil model^[13-16], most of these studies only rely on angle of repose as the evaluation index. The angle of internal friction and cohesion are the key soil parameters that affect the resistance of field operation. The internal friction and cohesion are added to the normal and tangential forces, and then the Hertz Mindlin model is used to calculate the particles to more comprehensively analyze the simulation parameters of grape cold soil. The internal friction angle and cohesion reflect the bearing capacity and friction performance of the soil. Adding them to the normal and tangential forces can be calculated by Hertz Mindlin model, which can more comprehensively analyze the simulation parameters^[4,17].

In this study, the soil characteristic parameters are studied by combining actual test and simulation test. In EDEM simulation, Hertz-Mindlin (no slip) is selected as the contact model^[18-20]. The methods of Plackett-Burman, steepest ascent, and Box-Behnken are used to analyze and optimize the experimental data. In order to provide a general parameter calibration method, the soil of Hongsipu in China is used for establishing of discrete element soil model, and the method will be used as a reference for constructing soil models for different soil types.

2 Materials and methods

2.1 Basic soil parameters

Soil samples are obtained from vineyard in northwest China at depth of 10-20 cm. The moisture content of soil is 9.29% obtained by the standard drying method, and the soil density is 1655 kg/m³ obtained by the cutting ring method. The cutting ring method is a traditional method to measure density. The particle size distribution and percentage content of soil are determined by the sieving method, as listed in Table 1. It can be seen from the table that the proportion of soil particle size greater than 2 mm is the least, and the proportion of particle size between 0.25-1.00 mm is the most. This indicates that the size of soil particle is small and the soil is sandy. Poisson's ratio and shear modulus are 0.35 and 2.89×10¹⁰ Pa respectively, according to the relevant literatures.

Table 1 Particle size distribution and percentage content of soil

Particle size/mm	>2	>1-2	>0.25-1	0.075-0.25	<0.075
Percentage/%	9.53	15.35	36.24	20.56	18.32

2.2 Direct shear stress test

In the direct shear stress test, the shear stress under different vertical pressures is measured by ZYY-4 direct shear preloading apparatus (Figure 1a) and ZJ strain controlled direct shear apparatus (Figure 1b). In the experiment, the speed of shearing is 0.8 mm/min and the maximum reading of the force measuring ring is recorded. Each group is repeated 3 times and the average value is calculated. The shear stress can be calculated as follows:

$$\tau = kR \tag{1}$$

where, τ is the shear stress of the specimen, kPa; k is the coefficient of the force measuring ring, kPa/0.01 mm; R is the reading of the dial indicator, 0.01 mm.

Taking shear strength τ_f as ordinate and normal stress σ as abscissa, the relationship between shear strength and normal stress is drawn. As shown in Figure 2, the inclination angle of the straight

line is the internal friction angle ϕ , and the intercept of the straight line on the ordinate is cohesion force c .

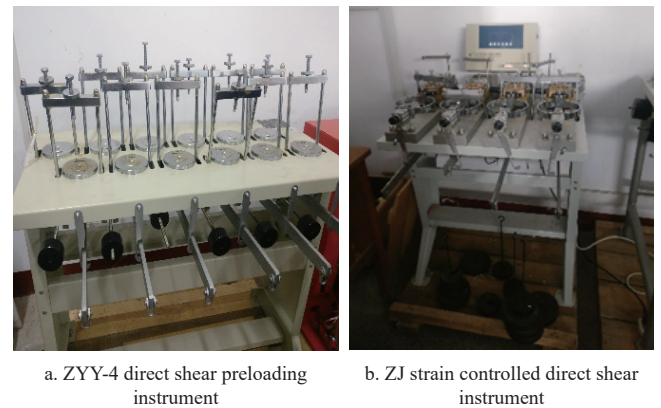


Figure 1 Experiment devices

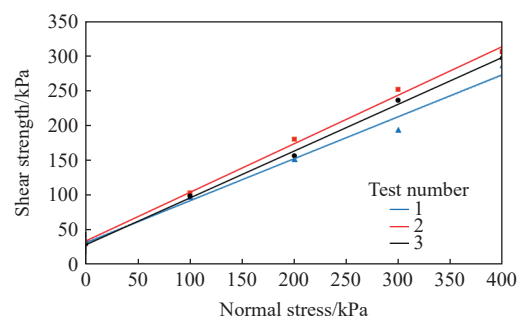


Figure 2 Relationship between shear stress and normal stress

It can be seen from the test data that the shear stress increases linearly with the increase of vertical stress in the case of a certain soil moisture content. The results show that the internal friction angle is 28.13° and the cohesion force is 32.31 kPa. The regression equation of shear strength and normal stress is in accordance with Equation (2), namely Mohr Coulomb theory equation^[21].

$$\tau_f = c + \sigma \tan \phi \tag{2}$$

2.3 Repose angle test

The repose angle is the maximum inclination angle between the side and the horizontal plane after the bulk materials are piled up. The funnel method is mainly used in the repose test, and the measurement test is shown in Figure 3. The soil is slowly added from the top of the funnel, and fall from the bottom of the funnel. As a result, the soil is piled up and formed a cone shape. The repose angle is measured by the digital inclinometer. The experiment is repeated 10 times and the average value is obtained. Finally, the repose angle is 32.28° by calculation.



Figure 3 Repose angle test

3 Calibration of particle simulation parameters

3.1 Contact model selection

There are many ways to bury the grape vine in Northwest China. The soil can be transferred by conveyor belt, rotary blade thrower, and plough scraper. The soil is broken under the action of shear, extrusion, and sliding. Only 9.53% of the soil with particle size greater than 2 mm was measured according to Section 1.1 of this paper, which proves that the soil is loose and the degree of hardening is small. Therefore, in order to truly reflect the soil characteristics, this study selected Hertz-Mindlin (no slip) as the particle contact model^[22].

Suppose that two spherical particles with radii R_1 and R_2 are in elastic contact, and the normal force F_n between them can be obtained by the following equation:

$$\begin{cases} F_n = \frac{4}{3}E^*(R^*)^{1/2}\alpha^{3/2} \\ \alpha = R_1 + R_2 - |r_1 - r_2| \\ \frac{1}{R^*} = \frac{1}{R_1} + \frac{1}{R_2} \\ \frac{1}{E^*} = \frac{1-\nu_1^2}{E_1} + \frac{1-\nu_2^2}{E_2} \end{cases} \quad (3)$$

where, E^* is the equivalent elastic modulus, MPa; R^* is the equivalent particle radius, mm; α is the normal overlap, mm; R_1 and R_2 are the position vectors of the spherical centers of the two particles; E_1, ν_1, E_2, ν_2 are the elastic modulus (kPa) and Poisson's ratio of particles 1 and 2, respectively.

The normal damping force F_n^d can be obtained as follows:

$$\begin{cases} F_n^d = -2\sqrt{\frac{5}{6}}\beta\sqrt{S_n m^* v_n^{rel}} \\ m^* = \frac{m_1 m_2}{m_1 + m_2} \\ v_n^{rel} = (v_1 - v_2) \times n \\ \beta = \frac{\ln e}{\sqrt{\ln^2 e + \pi^2}} \\ S_n = 2E^* \sqrt{R^* \alpha} \end{cases} \quad (4)$$

where, m^* is the equivalent mass, v_n^{rel} is the normal component of the relative velocity, β is the coefficient, S_n is the normal stiffness and E is the recovery coefficient. Suppose that the velocities of the two particles before collision are v_1, v_2 , and the normal unit vector of collision is n .

$$n = \frac{r_1 - r_2}{|r_1 - r_2|} \quad (5)$$

The tangential force F_t between particles can be calculated by the following equation:

$$\begin{cases} F_t = -S_t \delta \\ S_t = 8G^* \sqrt{R^* \alpha} \\ G^* = \frac{2-\nu_1^2}{G_1} + \frac{2-\nu_2^2}{G_2} \end{cases} \quad (6)$$

where, δ is the tangential overlap; S_t is the tangential stiffness; G^* is the equivalent shear modulus; G_1 and G_2 are the shear modulus of the two particles.

Tangential damping force F_t^d between particles can be calculated by the following equation:

$$F_t^d = -2\sqrt{\frac{5}{6}}\beta\sqrt{S_t m^* v_t^{rel}} \quad (7)$$

where, v_t^{rel} is the tangential relative velocity.

3.2 Range of contact parameters

The EDEM software has a granular material database module (GEMM). The company summarized a calculation method for particle parameter calibration based on the data accumulated in the past 20 many years. The value range of restitution coefficient, static friction coefficient, rolling friction coefficient between the soil particles, and surface energy of JKR can be obtained by inputting particle quantity, bulk density, and repose angle into GEMM database. The coefficient of restitution, static friction coefficient and dynamic friction coefficient between soil-soil and soil-45# steel are the key parameters of the EDEM simulation test^[23]. According to discrete element research literatures, soil density is 1655 kg/m³, Poisson's ratio is 0.35, and shear modulus is 2.89×10¹⁰ Pa. The remaining simulation parameter ranges are also determined by literature review, as listed in Table 2^[24-26].

Table 2 Range of simulation parameters

Symbol	Parameters	Low limit	High limit
X_1	Soil-soil restitution coefficient	0.15	0.75
X_2	Soil-soil static friction coefficient	0.20	0.90
X_3	Soil-soil rolling friction coefficient	0.05	0.20
X_4	Surface energy of soil for JKR model/(J·m ⁻²)	5	20
X_5	Soil-steel restitution coefficient	0.25	0.65
X_6	Soil-steel static friction coefficient	0.30	0.60
X_7	Soil-steel rolling friction coefficient	0.06	0.40
X_8-X_{11}	Blank parameters	—	—

3.3 Calibration method of simulation parameters

3.3.1 Design of Plackett-Burman method

After obtaining the value range of contact parameters, the Plackett-Burman method including 12 groups is designed by Design-expert software. Through repose angle simulation test and direct shear stress simulation test, as shown in Figure 4, the parameters with significant influence under each index are selected by taking repose angle, internal friction angle, and cohesion force as evaluation indexes. There are 7 parameters X_1-X_7 and 4 blank parameters X_8-X_{11} in the simulation test. Each parameter takes two levels of low and high, expressed by 1, -1.

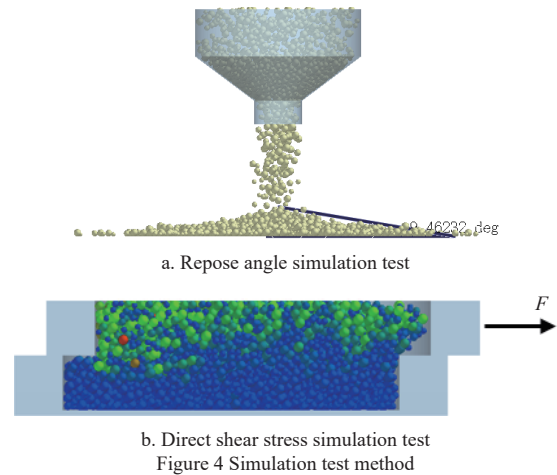


Figure 4 Simulation test method

In the repose angle simulation test, the size of funnel model is same as the actual size, the upper diameter is 24 cm and the lower diameter is 5 cm. A particle factory is established above the funnel to generate soil particles. The repose angle is measured by using the protractor in the post-processing module of EDEM software. In the

direct shear stress simulation test, the bottom area of soil sample is 30 cm² and the height is 2 cm. The upper box shears the soil at the speed of 0.8 mm/min, while applying different pressures on soil particles. The maximum transverse shear stress *F* is obtained in the EDEM software post-processing module. The cohesion force and internal friction angle are solved by combining the shear stress equation and Mohr Coulomb theory equation.

3.3.2 Design of steepest ascent method

The steepest ascent method is designed to determine the best value range of significant factors selected by Plackett-Burman method. According to the design scheme, as value of each significance factor increases with fixed step, the simulation results of repose angle, internal friction angle, and cohesion force are generated and compared with the actual values. The group whose result is closest to the actual result is selected as the center group and the two adjacent groups are selected as the high and low levels.

3.3.3 Design of Box-Behnken method

Based on the groups of parameters obtained from the steepest ascent test, this paper further analyzes the influence of different parameter combinations on the repose angle, cohesion force, and internal friction angle. Each significant factor is set at low, medium, and high levels, expressed as -1, 0, and +1. There are 17 groups of tests, of which 5 groups are at level 0.

4 Results and discussion

4.1 Results of Plackett-Burman method

Design-expert software is used to design 12 groups of Plackett-Burman method and record the results of each group, as listed in Table 3. Taking 11 parameters in Table 2 as test factors, repose angle, internal friction angle, and cohesion force as evaluation indexes. The data in Table 3 are analyzed by analysis of variance and the results are listed in Tables 4-6.

Table 3 Experimental design and results of Plackett-Burman

No.	X ₁	X ₂	X ₃	X ₄	X ₅	X ₆	X ₇	X ₈	X ₉	X ₁₀	X ₁₁	Repose angle/(°)	Internal friction angle/(°)	Cohesive force/kPa
1	-1	-1	-1	1	1	1	1	1	-1	1	-1	33.44	23.44	25.56
2	1	-1	1	-1	1	-1	1	1	-1	-1	1	48.09	28.09	30.21
3	1	1	1	1	-1	1	-1	1	-1	-1	-1	57.82	37.82	39.94
4	1	1	-1	-1	1	1	1	-1	1	-1	-1	54.24	34.24	36.36
5	-1	1	1	-1	-1	-1	1	1	1	1	-1	51.47	31.47	33.59
6	1	-1	-1	-1	-1	1	-1	1	1	1	1	46.52	25.52	28.64
7	1	1	-1	1	-1	-1	1	-1	-1	1	1	48.47	28.47	30.59
8	-1	1	-1	1	1	-1	-1	1	1	-1	1	50.19	30.19	32.31
9	1	-1	1	1	1	-1	-1	-1	1	1	-1	46.77	26.77	28.89
10	-1	1	1	-1	1	1	-1	-1	-1	1	1	53.02	33.02	35.14
11	-1	-1	1	1	-1	1	1	-1	1	-1	1	40.17	25.17	27.29
12	-1	-1	-1	-1	-1	-1	-1	-1	-1	-1	-1	40.55	20.55	22.67

Note: The variables X₁-X₁₁ are equal to those in Table 2. Same below.

Table 4 Significance analysis of parameters based on repose angle

Source	Sum of squares	df	Mean square	F-value	p-value
Model	489.841	7	69.977	15.545	0.0093**
X ₁	91.135	1	91.135	20.245	0.0108*
X ₂	296.709	1	296.709	65.9105	0.0012**
X ₃	47.720	1	47.720	10.600	0.0312*
X ₄	24.168	1	24.168	5.369	0.0814
X ₅	0.047	1	0.047	0.010	0.9236
X ₆	0.009	1	0.009	0.002	0.9663
X ₇	30.052	1	30.052	6.676	0.0611
Residual error	18.007	4	4.502		
Total	507.848	11			

Note: ** and * indicated significance at 0.01 and 0.05 levels, respectively. The same below.

Table 6 Significance analysis of parameters based on Cohesive force

Source	Sum of squares	df	Mean square	F-value	p-value
Model	245.716	7	35.102	11.694	0.015*
X ₁	27.210	1	27.210	9.065	0.039*
X ₂	166.284	1	166.284	55.396	0.0017**
X ₃	29.862	1	29.862	9.948	0.0344*
X ₄	0.343	1	0.343	0.114	0.7522
X ₅	2.755	1	2.755	0.918	0.3923
X ₆	17.934	1	17.934	5.975	0.0709
X ₇	1.327	1	1.327	0.442	0.5425
Residual error	12.007	4	3.002		
Total	257.723	11			

Note: df (degree of freedom) in the analysis of variance refers to the degree of freedom, which is an unrestricted number of variables when calculating a measurement system.

Table 5 Significance analysis of parameters based on internal friction angle

Source	Sum of squares	df	Mean square	F-value	p-value
Model	251.398	7	35.914	12.147	0.0147*
X ₁	24.282	1	24.282	8.212	0.0457*
X ₂	173.812	1	173.812	58.785	0.0016**
X ₃	33.100	1	33.100	11.195	0.0287*
X ₄	0.088	1	0.088	0.030	0.8711
X ₅	3.797	1	3.797	1.284	0.3204
X ₆	15.572	1	15.572	5.267	0.0834
X ₇	0.745	1	0.745	0.252	0.6421
Residual error	11.827	4	2.957		
Total	263.224	11			

It can be seen from Tables 4-6 that all models are significant, among which the Plackett-Burman model with repose angle as index showed the strongest significance. The results show that soil-soil restitution coefficient (X₁), soil-soil static friction coefficient (X₂), and soil-soil rolling friction coefficient (X₃) have significant effects on repose angle, internal friction angle, and cohesion force. Taking repose angle as the evaluation index, the order of significant factors is soil-soil static friction coefficient (X₂) > soil-soil restitution coefficient (X₁) > soil-soil rolling friction coefficient (X₃). Taking internal friction angle and cohesion force as evaluation indexes, the significance order is soil-soil static friction coefficient (X₂) > soil-soil rolling friction coefficient (X₃) > soil-soil restitution coefficient (X₁); other factors are not significant. Therefore, soil-soil

restitution coefficient (X_1), soil-soil static friction coefficient (X_2), and soil-soil rolling friction coefficient (X_3) are selected for further research.

4.2 Results of steepest ascent method

Based on results of Plackett-Burman method, soil-soil restitution coefficient (X_1), soil-soil static friction coefficient (X_2) and soil-soil rolling friction coefficient (X_3) are selected as independent variables. The value range of each parameter is set in five levels. The results of steepest ascent test are listed in Table 7. At No.4, the values of repose angle, internal friction angle, and cohesion force are close to the actual values, which indicates that optimal value of parameters is near No.4. Therefore, No.4 is selected as the central point, No.3 and No.5 are selected as low and high levels respectively. The other non-significant parameters are determined according to references^[27], so soil-steel static friction coefficient is 0.38, soil-steel rolling friction coefficient is 0.37, and soil-steel restitution coefficient is 0.60.

4.3 Results of Box-Behnken response surface method

In order to further research, repose angle (Y_1), internal friction angle (Y_2), and cohesion force (Y_3) are integrated into a comprehensive evaluation index. The value of evaluation index is calculated by Hassan method, so that the index is expressed as the

Table 7 Design and results of steepest ascent test

No.	A	B	C	Repose angle/(°)	Internal friction angle/(°)	Cohesive force/kPa
1	0.15	0.2	0.05	10.84	12.83	11.32
2	0.30	0.375	0.0875	22.63	19.21	17.14
3	0.45	0.55	0.125	28.98	24.62	25.45
4	0.60	0.725	0.1625	34.98	29.73	32.61
5	0.75	0.9	0.2	41.73	36.54	40.22

Note: Parameter A, B, and C are equal to parameters X_5 , X_6 , and X_7 , respectively. The same as below.

"normalized value" (Y), and the range of value is $0-1^{[28-30]}$. The calculation equation is

$$\begin{cases} d_i = \frac{Y_i - Y_{min}}{Y_{max} - Y_{min}} \\ Y = (d_1 d_2 \dots d_k)^{1/k} \end{cases} \quad (8)$$

where, Y_i is the index value, Y_{min} and Y_{max} are the minimum and maximum values of all values obtained by each factor at different levels, and k is the number of indicators.

The results of Box-Behnken method are listed in Table 8. Design-expert software is used to establish the second-order regression model of three parameters and evaluation index.

Table 8 Design and results of Box-Behnken test

No.	Parameter A	Parameter B	Parameter C	Repose angle Y_1 /(°)	Internal friction angle Y_2 /(°)	Cohesive force Y_3 /kPa	Evaluation index Y
1	0.6(0)	0.725(0)	0.1625(0)	35.97	35.27	33.86	0.91
2	0.75(1)	0.725(0)	0.2(1)	31.34	26.63	36.61	0.49
3	0.45(-1)	0.55(-1)	0.1625(0)	28.32	35.59	23.14	0
4	0.6(0)	0.55(-1)	0.2(1)	31.78	29.01	23.16	0.07
5	0.6(0)	0.9(1)	0.2(1)	32.19	31.23	23.54	0.22
6	0.45(-1)	0.725(0)	0.2(1)	30.95	30.21	30.28	0.5
7	0.6(0)	0.725(0)	0.1625(0)	36.11	35.41	36.16	0.98
8	0.6(0)	0.55(-1)	0.125(-1)	26.34	32.54	29.24	0
9	0.6(0)	0.725(0)	0.1625(0)	35.88	35.86	35.55	0.97
10	0.45(-1)	0.725(0)	0.125(-1)	35.62	26.15	30.71	0.41
11	0.6(0)	0.9(1)	0.125(-1)	36.21	24.73	29.88	0
12	0.75(1)	0.9(1)	0.1625(0)	31.56	31.42	23.52	0.21
13	0.75(1)	0.725(0)	0.125(-1)	38.21	28.34	23.37	0.19
14	0.6(0)	0.725(0)	0.1625(0)	36.02	34.89	34.57	0.92
15	0.45(-1)	0.9(1)	0.1625(0)	32.15	30.32	25.05	0.35
16	0.75(1)	0.55(-1)	0.1625(0)	30.21	27.28	26.71	0.29
17	0.6(0)	0.725(0)	0.1625(0)	35.98	35.53	36.60	0.99

$$Y = -18.8137 + 12.4924A + 27.0763B + 73.0083C - 4.0952AB + 9.3333AC + 5.7143BC - 9.2556A^2 - 17.4122B^2 - 247.6444C^2.$$

The results of variance analysis of the regression model are listed in Table 9. The results show that the p -value of the model is less than 0.0001, indicating that the model is extremely significant. The p -value is a measure of difference. The p -value for lack of fit is greater than 0.05, indicating that the model fits well. The determination coefficient (R^2) is 0.9882 and the adjusted determination coefficient (R^2_{adj}) is 0.9731. They can show that the fitting model is reliable, and the key parameters of soil can be accurately analyzed and predicted by the model. From the variance analysis of the fitted regression model, it can be seen that A, B, C, AB, A^2 , B^2 , and C^2 have significant influence on evaluation index (Y) in the given range of various factors. In the first term of the regression equation, soil-soil static friction coefficient (B), soil-soil rolling friction coefficient (C) and soil-soil restitution coefficient (A) have significant influence on evaluation index, and the order of influence of each factor is $B > C > A$. In the interaction term, AB is

Table 9 Variance analysis of regression model

Source	Sum of squares	df	Mean square	F-value	p-value
Model	2.219	9	0.247	65.324	<0.0001**
A	0.135	1	0.135	35.828	0.0006**
B	0.898	1	0.898	237.820	<0.0001**
C	0.304	1	0.304	80.439	<0.0001**
AB	0.046	1	0.046	12.247	0.0100*
AC	0.011	1	0.011	2.921	0.1312
BC	0.006	1	0.006	1.490	0.2617
A^2	0.182	1	0.183	48.381	0.0002**
B^2	1.197	1	1.197	317.222	<0.0001**
C^2	0.511	1	0.511	135.296	<0.0001**
Residual error	0.026	7	0.004		
Lack of fit	0.021	3	0.007	5.288	0.0653
Pure error	0.005	4	0.001		
Total	2.245	16			
$R^2=0.9882$					
$R^2_{adj}=0.9731$					

the significant influence on evaluation index, AC and BC are not significant, indicating that the interaction between soil-soil restitution coefficient (A) and soil-soil static friction coefficient (B) is very obvious. In the quadratic term, A^2 , B^2 and C^2 have extremely significant effects on evaluation index, which indicates that the influence of A , B , and C on evaluation index is nonlinear.

4.4 Optimal soil parameters

The influence of interaction among A , B , and C on evaluation index is shown in Figure 5. When the comprehensive evaluation index (Y) is 1, the optimal soil parameters can be obtained by

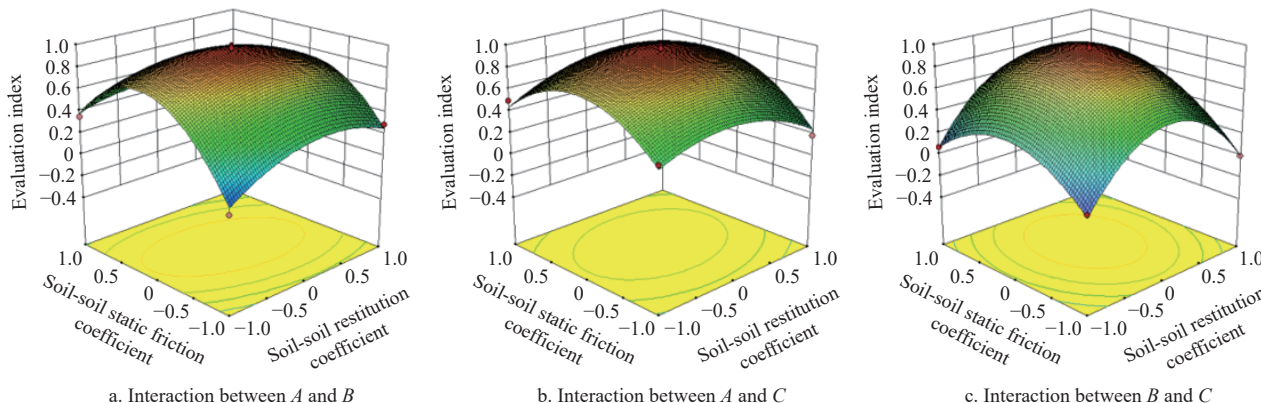


Figure 5 Response surface diagram of Soil-soil restitution coefficient (A), Soil-soil static friction coefficient (B), and Soil-soil rolling friction coefficient (C) for their mutual interaction

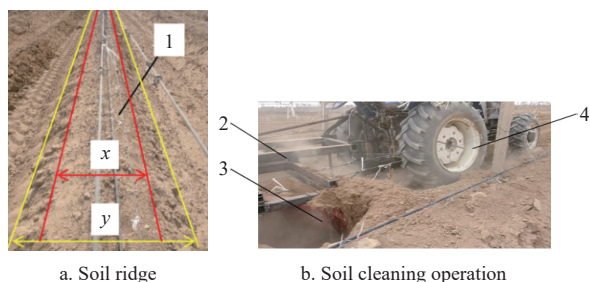
4.5 Experimental verification

4.5.1 Purpose and method

In order to further verify whether the simulation parameters obtained by repose angle test and direct shear stress test consistent with the real soil, this paper compares field test and simulation test of soil cleaning. In the actual process of soil cleaning, from the macro view, the soil appears cracking, sliding and other states under the action of the scraper. From the micro view, the bonding bond between soil particles limiting the normal and tangential forces of particles is damaged by force. The scraper is used to clean the soil on both sides of the ridge. Due to the effect of shear and extrusion on the soil ridge, the soil ridge collapse after the completion of the soil cleaning operation. However, different characteristics of soil will present different collapsing results. For example, the loose soil collapses easily, while the hardened soil is hard to collapse. Therefore, the height of the remaining soil ridge after soil cleaning operation is taken as the evaluation standard, and the measured value is compared with the simulated value. The error of them are used to judge the correctness of the parameters of soil.

4.5.2 Field test of soil cleaning

The cross section of soil ridge is isosceles trapezoid and its upper width (x) is 80 cm, lower width (y) is 120 cm and height is 60 cm, as shown in Figure 6a. The size of scraper is that the length



1. Soil ridge 2. Frame 3. Scraper 4. Tractor

Figure 6 Field test

response surface. The values of A , B , and C corresponding to the highest point of the response surface are the values of the optimal parameters. Figure 5 shows that soil-soil restitution coefficient is 0.596, soil-soil static friction coefficient is 0.725, and soil-soil rolling friction coefficient is 0.162. Under optimal parameters, the simulation results show that the repose angle is 31.97° , the internal friction angle is 27.61° , and the cohesion force is 33.06 kPa. The relative errors with the actual values are 9.54%, 1.87%, and 2.31%. It indicates that the fitting model is reliable and the calibrated parameters are accurate.

is 140 cm, height is 60 cm and the radius of curved surface is 40 cm. The depth of the scraper into ridge is 30 cm, and the inclination angle of the scraper is 45° . In the field test, the forward speed of the machine is 5 km/h and the scraper cleans the soil on both sides of the ridge. The operation process is shown in Figure 6b. The height of soil ridge is measured at marked points that are randomly selected after test and the average value is used as the final result.

4.5.3 Simulation test of soil cleaning

The discrete element method is used for simulation test. The simulation area is established in EDEM software and its size is 5 m×5 m (length×width). The size of the soil ridge is consistent with the actual soil ridge. In simulation process, the soil parameters are all the optimal parameters obtained. The generated model of soil ridge is shown in Figure 7a.

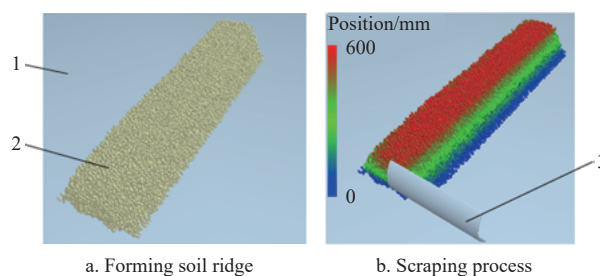


Figure 7 Simulation test

The model of scraper is drawn by Solidworks software and imported into EDEM software. The material of scraper is Q235 steel, the density is 7850 kg/m^3 , Poisson's ratio is 0.28 and the shear modulus is $8.2 \times 10^{10} \text{ Pa}$, respectively^[31]. In the process of soil cleaning, there is relative movement between soil and Q235 steel. According to literatures^[32], static friction coefficient, rolling friction coefficient and restitution coefficient between soil particles and Q235 steel are 0.38, 0.37, and 0.60, respectively. The forward speed of scraper is 5 km/h. The depth of scraper into ridge and the

inclination angle of scraper are consistent with the actual status. In the EDEM simulator module, the time step is 0.000 001 s and the data storage interval is 0.05 s. The total simulation time is 24 s, in which 0-20 s is the modeling time of soil ridge, 20-24 s is operation time of the scraper. In the post-processing of EDEM software, the position of particle in the Z-axis is taken as the measurement basis of the soil ridge height. Five marked points in the stable stage of soil cleaning are randomly selected to measure the height of soil ridge, and the average value is taken as the final result.

4.5.4 Results and analysis

The measurements of height of soil ridge after soil cleaning are shown in Figure 8. Table 10 shows that the error of height between simulation test and field test is 4.06% and the error is within the acceptable range. It can be concluded that the method of taking the repose angle, internal friction angle and cohesion force as evaluation indexes to calibrate the key parameters of soil is accurate and reliable.



Figure 8 Field measurement

Table 10 Comparison of ridge height between simulation test and field test

Parameter	Measured value/mm	Simulation value/mm	Error/%
Height of soil ridge	56.95	54.64	4.06

5 Conclusions

Based on the soil characteristics in Central Asia, this paper determined the soil parameters by using the method of combining actual test with simulation test. Hertz-Mindlin (no slip) contact model is used to carry out repose angle test and direct shear stress test. Plackett-Burman method, steepest climbing method, and Box-Behnken method are used to analyze and optimize the experimental data. Taking the soil of Northwest China as an example, field test is carried out to verify the accuracy of the simulation, and finally, determine the simulation parameters of soil. The conclusions are as follows:

1) According to the range of contact parameters, Plackett-Burman method is designed by using Design-expert software. Through the repose angle test and direct shear stress test, taking the repose angle, internal friction angle, and cohesion force as indexes, the results show that soil-soil restitution coefficient, soil-soil static friction coefficient, and soil-soil rolling friction coefficient are significant, and the other parameters are not significant.

2) According to the significant factor selected by Plackett-Burman method, steepest ascent method is designed to further narrow the range of value. The best range of significance factors is that soil-soil restitution coefficient is 0.45-0.75, soil-soil static friction coefficient is 0.55-0.90 and soil-soil rolling friction

coefficient is 0.125-0.200. Each significance factor iteratively increases in accordance with the fixed step.

3) The results of Box-Behnken method show that the soil-soil static friction coefficient, soil-soil rolling friction coefficient, and soil-soil restitution coefficient have significant influence in the first term. The interaction between soil-soil restitution coefficient and soil-soil static friction coefficient is significant. The optimal soil parameters: soil-soil restitution coefficient is 0.596, soil-soil static friction coefficient is 0.725, and soil-soil rolling friction coefficient is 0.162.

4) The accuracy of parameters is verified by comparing the field test with the simulation test. The results show that the error between the simulation soil model and the actual soil is 4.06%, and the error is within the acceptable range. This study proposed a calibrated method of soil simulation parameters based on repose angle test and direct shear stress test. This method can quickly and accurately find the target parameters and provide a way for EDEM simulation to establish soil model.

Acknowledgements

This work was financially supported by the National Science and Technology Major Project of China (Grant No. 2019YFD1002502); the National Natural Science Foundation of China (Grant No. 51 675 239); The Natural Science Fund Project of Colleges in Jiangsu Province of China (Grant No. 19KJA430018); The Important Development Program of Ningxia Province of China (Grant No. 2018BBF02020); The Research and Development Program of Zhenjiang Province of China (Grant No. NY2019015).

[References]

- [1] Jaeger H M, Nagel S R, Behringer R P. The physics of granular materials. *Physics Today*, 1996; 49(4): 32–38.
- [2] Ucgul M, Fielke J M, Saunders C. Three-dimensional discrete element modelling of tillage: determination of a suitable contact model and parameters for a cohesionless soil. *Biosystems Engineering*, 2014; 121(3): 105–117.
- [3] Li B, Chen Y, Chen J. Modeling of soil-claw interaction using the discrete element method (DEM). *Soil & Tillage Research*, 2016; 158: 177–185.
- [4] Tamás K, Jóri I J, Mouazen A M. Modeling soil sweep interaction with discrete element method. *Soil & Tillage Research*, 2013; 134(8): 223–231.
- [5] Smith W, Peng H. Modeling of wheel-soil interaction over rough terrain using the discrete element method. *Journal of Terramechanics*, 2013; 50(5): 277–287.
- [6] Briend R. Modelling wheel-soil interactions using the discrete element method for tread shape optimization. Montreal: McGill University, 2010.
- [7] Hu J P, Xu G H, Shi Y J, Wu L B. A numerical simulation investigation of the influence of rotor wake on sediment particles by computational fluid dynamics coupling discrete element method. *Aerospace Science and Technology*, 2020; 105: 106046.
- [8] Ucgul M, Fielke J M, Saunders C. 3D DEM tillage simulation: Validation of a hysteretic spring (plastic) contact model for a sweep tool operating in a cohesionless soil. *Soil and Tillage Research*, 2014; 144: 220–227.
- [9] Ucgul M, Fielke J M, Saunders C. Defining the effect of sweep tillage tool cutting edge geometry on tillage forces using 3D discrete element modelling. *Information Processing in Agriculture*, 2015; 2(2): 130–141.
- [10] Chen Y, Munkholm L J, Nyord T. A discrete element model for soil-sweep interaction in three different soils. *Soil and Tillage Research*, 2013; 126: 34–41.
- [11] Wu T, Huang W F, Chen X S, Ma X, Han Z Q, Pan T. Calibration of discrete element model parameters for cohesive soil considering the cohesion between particles. *Journal of South China Agricultural University*, 2017; 38(3): 93–98. (in Chinese)
- [12] Xiang W, Wu M L, Lv J N, Quan W, Ma L, Liu J J. Calibration of simulation physical parameters of clay loam based on soil accumulation test. *Transactions of the CSAE*, 2019; 35(12): 116–123. (in Chinese)
- [13] Li B, Liu F Y, Mu J Y, Chen J, Han W T. Distinct element method analysis

- and field experiment of soil resistance applied on the subsoiler. *Int J Agric & Biol Eng*, 2014; 7(1): 54–59.
- [14] Qi J T, Meng H W, Kan Z, Li C S, Li Y P. Analysis and test of feeding performance of dual-spiral cow feeding device based on EDEM. *Transactions of the CSAE*, 2017; 33(24): 65–71. (in Chinese)
- [15] Gao G H, Ma S. Improvement of transplanting manipulator for potted flower based on discrete element analysis and Su-field analysis. *Transactions of the CSAE*, 2017; 33(6): 35–42. (in Chinese)
- [16] Fernandez J W, Cleary P W, McBride W. Effect of screw design on hopper drawdown of spherical particles in a horizontal screw feeder. *Chemical Engineering Science*, 2011; 66(22): 5585–5601.
- [17] Shi L R, Zhao W Y, Sun W. Parameter calibration of soil particles contact model of farmland soil in northwest arid region based on discrete element method. *Transactions of the CSAE*, 33(21): 181–187. (in Chinese)
- [18] Brove E L, Tijssens E, Miguel H S, Gonzalez C O, Ramon H. Prediction model for non-inversion soil tillage implemented on discrete. *Computers and Electronics in Agriculture*, 2014; 106(5): 120–127.
- [19] Shmulevich I. State of the art modeling of soil-tillage interaction using discrete element method. *Soil & Tillage Research*, 2010; 111: 41–53.
- [20] Briend R, Radziszewski P, Pasini D. Virtual soil calibration for wheel-soil interaction simulations using the discrete-element method. *Canadian Aeronautics & Amp Space Journal*, 2011; 57(1): 59–64.
- [21] Ucgul M, Fielke J M, Saunders C. Three-dimensional discrete element modelling (DEM) of tillage: accounting for soil cohesion and adhesion. *Biosystems Engineering*, 2015; 129(5): 298–306.
- [22] Wang G Q, He W J, Wang J X. *Discrete element method and its application in EDEM*. Xi'an: Xi'an Technological University Press, 2010; 155p. (in Chinese)
- [23] Shi L R, Zhao W Y, Yang X P. Effects of typical corn kernel shapes on the forming of repose angle by DEM simulation. *Int J Agric & Biol Eng*, 2022; 15(2): 248–255.
- [24] Shi L R, Yang X P, Zhao W Y, Sun W, Wang G P, Sun B G. Investigation of interaction effect between static and rolling friction of corn kernels on repose formation by DEM. *Int J Agric & Biol Eng*, 2021; 14(5): 238–246.
- [25] Dai F, Song X F, Zhao W Y, Shi R J, Zhang F W, Zhang X K. Mechanism analysis and performance improvement of mechanized ridge forming of whole plastic film mulched double ridges. *Int J Agric & Biol Eng*, 2020; 13(5): 107–116.
- [26] Zhu Y H, Xia J F, Zeng R, Zhen K, Du J, Liu Z Y. Prediction model of rotary tillage power consumption in paddy stubble field based on Discrete Element Method. *Transactions of the CSAM*, 2020; 51(10): 42–50. (in Chinese)
- [27] Wu W, Cui G H, Lu B. Optimization of multiple evariables: Application of central composite design and overall desirability. *Chinese Pharmaceutical Journal*, 2000; 35(8): 530–533. (in Chinese)
- [28] Wang Y, Lv L Y, Li Y, He J P, Xiao R M, Yang K, et al. Optimization of Yi medicine processing technology for honeyed wine rhubarb by Box-behnken design response surface methodology. *Chinese Traditional and Herbal Drugs*, 2019; 50(4): 844–851. (in Chinese)
- [29] Huang Y H, Li D T. Optimization of purification process of *Platycladus orientalis* leaves by Plackett-Burman test combined with central composite design response surface methodology. *Traditional Chinese Medicine*, 2020; 43(3): 682–686. (in Chinese)
- [30] Liu W Z, He J, Li H W, Li X Q, Zheng K, Wei Z C. Calibration of simulation parameters for potato minituber based on EDEM. *Transactions of the CSAM*, 2018; 49(5): 125–135. (in Chinese)
- [31] Ma S, Xu L M, Yuan Q C, Niu C, Zeng J, Chen C, et al. Calibration of discrete element simulation parameters of grapevine anti-freezing soil and its interaction with soil-cleaning components. *Transactions of the CSAE*, 2020; 36(1): 40–49. (in Chinese)
- [32] Ucgui M, Saunders C, Fielke J M. Discrete element modelling of top soil burial using a full scale mouldboard plough under field conditions. *Biosystems Engineering*, 2017; 160: 140–153.